Development 138, 273-282 (2011) doi:10.1242/dev.051680

FGF10 controls the patterning of the tracheal cartilage rings via *Shh*

Frédéric G. Sala[1], Pierre-Marie Del Moral[1], Caterina Tiozzo[1], Denise Al Alam[1], David Warburton[1], Tracy Grikscheit[1], Jacqueline M. Veltmaat[1,*] and Saverio Bellusci[1,2,†]

SUMMARY

During embryonic development, appropriate dorsoventral patterning of the trachea leads to the formation of periodic cartilage rings from the ventral mesenchyme and continuous smooth muscle from the dorsal mesenchyme. In this work, we have investigated the role of two crucial morphogens, fibroblast growth factor 10 and sonic hedgehog, in the formation of periodically alternating cartilaginous and non-cartilaginous domains in the ventral mesenchyme. Using a combination of gain- and loss-of-function approaches for FGF10 and SHH, we demonstrate that precise spatio-temporal patterns and appropriate levels of expression of these two signaling molecules in the ventral area are crucial between embryonic day 11.5 and 13.5 for the proper patterning of the cartilage rings. We conclude that the expression level of FGF10 in the mesenchyme has to be within a critical range to allow for periodic expression of *Shh* in the ventral epithelium, and consequently for the correct patterning of the cartilage rings. We propose that disturbed balances of *Fgf10* and *Shh* may explain a subset of human tracheomalacia without tracheo-esophageal fistula or tracheal atresia.

KEY WORDS: *Fgf10*, *Shh*, Trachea, Cartilage formation, Mouse

INTRODUCTION

The mouse trachea starts to develop at E9.5 from the laryngotracheal groove, a ventral outgrowth of the foregut endoderm into the surrounding mesoderm. This structure elongates to form a tube extending from the larynx to the two main bronchi of the lung. Although the endoderm differentiates into a ciliated pseudo-stratified epithelium, the mesenchyme on the ventral side of the trachea matures progressively into C-shaped cartilage rings that maintain patency of the lumen, while the dorsal mesenchyme differentiates into smooth muscle. Proper periodic development of the tracheal cartilage ring is crucial for normal breathing, as the rings provide support to the trachea lumen by limiting its expansion during inhalation and preventing its collapse upon exhalation.

Tracheal malformations in human involving cartilage defects can be grouped into two classes (for a review, see Kay and Goldsmith, 2006). Malformations in the first class are characterized by an almost continuous tracheal cartilaginous sleeve involving multiple cartilage rings. In extreme cases, one single ring throughout the entire length of the trachea can be observed. This defect can be associated with tracheal stenosis, which is a narrowing of the lumen of the trachea (Ho and Koltai, 2008). The second class of defects is tracheomalacia**,** where the cartilage rings are too floppy, resulting in weakness of the tracheal walls leading to an eventual collapse of these walls (Austin and Ali, 2003). Depending on the severity of these tracheal cartilage defects, lethal alteration of respiratory function can be observed. Unfortunately, outcomes of reparative surgery for these malformations are often unsatisfactory. There is therefore a need to expand our knowledge on the molecular bases of tracheal cartilage formation to design novel approaches to ameliorate cartilage formation.

A few regulators of cartilage formation are known (Goldring et al., 2006) and most of these molecules seem to converge at the level of the transcription factor SOX9. For example, β-catenin in the mesenchyme interacts with SOX9 to regulate the differentiation of the chondroprogenitor cells (Akiyama et al., 2004). Bone morphogenetic protein 4 (BMP4) induces differentiation of the mesenchymal cells into chondroprogenitors via SOX9 (Hatakeyama et al., 2004). Moreover, impaired BMP signaling induces esophageal atresia and tracheo-esophageal fistula with extensive defects in tracheal cartilage ring formation (Que et al., 2006). Sonic hedgehog (SHH) also induces cartilage differentiation via activation of SOX9 (Park et al., 2010), and partial inactivation of *Shh* results in tracheo-bronchial cartilage ring abnormalities (Miller et al., 2004). Finally, fibroblast growth factor (FGF) family members such as *Fgf4* and *Fgf8* have been described to play an important role during cartilage formation (Goldring et al., 2006). Recently, we demonstrated that FGF10 causes the formation of a uniform cartilaginous sleeve in the trachea, when it activates ectopically expressed FGFR2B in the mesenchyme, reminiscent of the anomaly observed in humans with Apert syndrome (Tiozzo et al., 2009).

In this study, we further determined the normal role of mesenchymal FGF10, signaling via FGFR2B in the epithelium, in tracheal cartilage formation in the mouse embryo. We demonstrate that proper levels of mesenchymal *Fgf10* expression between E11.5 and E13.5 are crucial for the induction of a periodic pattern of *Shh* expression in the ventral epithelium, and for the correct patterning of the cartilage rings downstream of *Shh* signaling. Deregulation of the expression of one of these two morphogens during this critical time window could therefore be a novel mechanism for abnormal cartilage ring formation in humans.

[1]Developmental Biology and Regenerative Medicine Program, Saban Research Institute of Childrens Hospital Los Angeles, Los Angeles, CA 90027, USA. [2]University of Giessen Lung Center, Excellence Cluster in Cardio-Pulmonary Systems, Department of Internal Medicine II, Klinikstrasse 36, 35392 Giessen, Germany.

*Present address: A*STAR Institute of Molecular and Cell Biology, 61 Biopolis Drive, Proteos, 138673, Singapore
†Author for correspondence (sbellusci@chla.usc.edu)

Accepted 8 November 2010

MATERIALS AND METHODS

Mice

Fgf10$^{+/-}$ mice (Sekine et al., 1999) were maintained on a C57BL/6 background. *Topgal* mice (DasGupta and Fuchs, 1999) were maintained on a mixed background. These strains were intercrossed to obtain [*Fgf10*$^{-/-}$*;Topgal*] embryos. The *Fgf10*$^{Mlcv\text{-}nlacZ\text{-}v24}$ mice (Kelly et al., 2001) (hereafter called *Fgf10*^{lacZ}) were maintained on a mixed agouti background. *Dermo-1*$^{Cre/+}$ mice (Yu et al., 2003), on a C57BL6 background, were crossed with *rtTA*$^{flox/flox}$ (Belteki et al., 2005) and *tet(O)Fgf10* mice (Clark et al., 2001), on a mixed background, to generate [*Dermo-1*$^{Cre/+}$*;rtTA*$^{flox/flox}$*; tet(O)Fgf10*] (hereafter tet(O)*Fgf10*^{Dermo1}) embryos. *Ttf-1*$^{Cre/+}$ (also known as *Nkx2.1*^{Cre}) mice (Tiozzo et al., 2009), on a 129P3/J background, were crossed with *rtTA*$^{flox/flox}$ and *tet(O)Shh* mice (Miller et al., 2004), on a 129P3/J background, to generate [*Ttf-1*$^{Cre/+}$*;rtTA*$^{flox/flox}$*;tet(O)Shh*] (hereafter *tet(O)Shh*$^{Ttf\text{-}1}$) embryos. *Ttf-1*^{Cre} mice were crossed with *Shh*$^{flox/flox}$ mice (The Jackson Laboratory) to generate (F2) [*Ttf-1*$^{Cre/+}$*; Shh*$^{flox/flox}$] embryos. *Ttf-1*^{Cre} mice were crossed with *Rosa26* reporter line (B6.129S4-*Gt(ROSA)26Sor*^{tm1Sor}/J, The Jackson Laboratory) to follow the expression pattern of the *Ttf-1* promoter.

Induction of the rtTA/tet(O) system

Timed pregnant mice were fed with doxycycline chow (Rodent diet with 0.0625% doxycycline, Harlan Teklad TD01306) at specific gestational stages.

Whole-mount in situ hybridization

Tracheas were isolated from the embryos and fixed for 2 hours in 4% paraformaldehyde (PFA) in PBS at 4°C. The samples were washed twice in PBS for 5 minutes, transferred in 70% ethanol overnight and stored in 100% ethanol until needed. Whole-mount in situ hybridization was performed as described (Winnier et al., 1995) with riboprobes transcribed from murine cDNA templates encoding a cDNA fragment of 584 bp for *Fgf10* (Bellusci et al., 1997), 622 bp for *Fgfr2b* cDNA and 642 bp for *Shh* (both kind gifts from Dr Andrew McMahon, Harvard University, Boston, MA), 500 bp for *Sox9* (a kind gift from Brigid Hogan, Duke University, Durham, NC, USA) and 1.5 kb for *Bmp4* (Winnier et al., 1995).

Measurement of pixel intensity of the whole-mount in situ hybridization signal

In photographs of tracheas stained by whole-mount in situ hybridization with specific probe for *Shh*, lines were drawn in the ventral and dorsal epithelial domain of *Shh* expression, parallel to the outer surface of the trachea. Along these lines, pixel intensity of the in situ hybridization signal was measured and graphs were generated using the Leica AF6000 software.

lacZ staining

Samples were briefly fixed in 4% PFA. *lacZ* expression on *Fgf10*^{lacZ} and *Topgal* tracheas was monitored by β-galactosidase activity using 1 mg X-gal/ml dimethylformamide in 5 mM $K_3Fe(CN)_6$/5 mM $K_4Fe(CN)_6$/2 mM $MgCl_2$ in D-PBS (pH 7.4).

Proliferation analysis

Two pregnant females were injected at the 13th day of pregnancy with 0.2 ml of bromodeoxyuridine (BrdU, Amersham Biosciences, UK) 20 minutes before sacrifice. The first female carried one mutant (M1). The second female carried two mutants (M2 and M3). Mutant M1 was compared with its own wild-type littermate control, and mutants M2 and M3 were compared with their own wild-type littermate controls.

The tracheas were dissected from the embryos, preserved in 4% PFA solution, paraffin embedded and sectioned at 5 μm. The sections were then incubated with monoclonal anti-bromodeoxyuridine (Clone BU-1) RPN 202 as recommended by the manufacturer (Amersham Biosciences), followed by Cy3-labeled anti-mouse secondary antibodies (Jackson ImmunoResearch). Slides were mounted with Vectashield containing DAPI. The sections were photographed using an epi-fluorescence photo-microscope (Leica, DM4000). Proliferation rate was determined as the number of BrdU-positive cells per total number cells (average of 400 cells counted per section) in epithelium and mesenchyme. For analysis of statistical significance, we have considered the three mutant tracheas and their corresponding controls as three pairs and performed a two-tail paired *t*-test on the data.

Immunostaining

The tracheas were fixed in 4% PFA, paraffin embedded and sectioned at 5 μm. Antigen was retrieved by boiling the slides using a microwave for 20 minutes in 10 mM sodium citrate (pH 6.0). The slides were incubated overnight at 4°C with the following primary antibodies: type II collagen (1/40, Chemicon International), β-tubulin (1/100, BioGenex) and rabbit anti-pro-SP-C (kindly provided by Dr J. Whitsett). Cy3- or FITC-conjugated secondary antibodies were used. Slides were mounted with Vectashield containing DAPI.

Histological staining

Cross-sections (5 μm) were stained with Hematoxylin and Eosin according to standard procedures or with Alcian Blue as described previously (see http://www.ihcworld.com/_protocols/special_stains/alcian_blue.htm).

RESULTS

Fgf10 and *Fgfr2b* are expressed early during trachea development in the mouse

Expression of *Fgf10* was investigated between E11.5 and E18.5 using whole-mount in situ hybridization of wild type, and *lacZ* staining of *Fgf10*^{lacZ} tracheas. We were not able to detect *Fgf10* expression at E11.5 (data not shown). In E12.5-E14.5 embryos, we could not identify any *lacZ* staining in *Fgf10*^{lacZ} reporter mice (data not shown), and needed to develop the in situ hybridization signal for 12 hours at room temperature, suggesting that the expression level of *Fgf10* is very low at these stages (Fig. 1A-C). Although *Fgf10* expression is initially expressed uniformly in the ventral mesenchyme at E12.5 and E13.5 (Fig. 1A,B, respectively), it becomes progressively regionalized in a periodic pattern, as seen at E14.5 (Fig. 1C) and E16.5 (Fig. 1D and the corresponding sagittal section shown in 1E). From E12.5 to E16.5, *Fgf10* is not expressed in the dorsal mesenchyme of the trachea (Fig. 1A-E). Analysis of whole-mount *Fgf10*^{lacZ} tracheas (Fig. 1F,G) and frontal and transversal vibratome sections thereof (Fig. 1H,H′) at E18.5 confirmed the restriction of *Fgf10* expression to the ventral side and in between the cartilage rings at that late stage as well.

As FGFR2B is the main receptor for FGF10 (De Moerlooze et al., 2000; Ohuchi, 2000), its expression pattern was also investigated between E12.5 and E14.5 using whole-mount in situ hybridization. At all stages, *Fgfr2b* is uniformly expressed in the epithelium of the trachea (Fig. 1I-K), strongly suggesting that mesenchymal FGF10 can evoke signaling in the tracheal epithelium via activation of this receptor.

Fgf10 inactivation results in a shortened trachea with severe defects in patterning of the cartilage rings

In order to follow the formation of the cartilage rings during tracheal development, we determined the expression of type II collagen, an early marker of cartilage differentiation (Sandell et al., 1994). At E11.5, type II collagen is expressed only in the lamina propria at the ventral side of the wild-type trachea (Fig. 2A). The staining expands into the ventral mesenchyme by E12.5 (Fig. 2B). At E13.5, the onset of periodicity in type II collagen expression becomes visible (Fig. 2C), and is fully determined by E14.5 (Fig. 2D). Thus, the patterning of the tracheal cartilage is progressively established, starting at E13.5 and defined by E14.5 in wild-type embryos. In the *Fgf10*$^{-/-}$ trachea, the expression of type II collagen appears normal at E11.5 and E12.5 (Fig. 2E,F). The first defect is observed at E13.5 when collagen expression fails to become

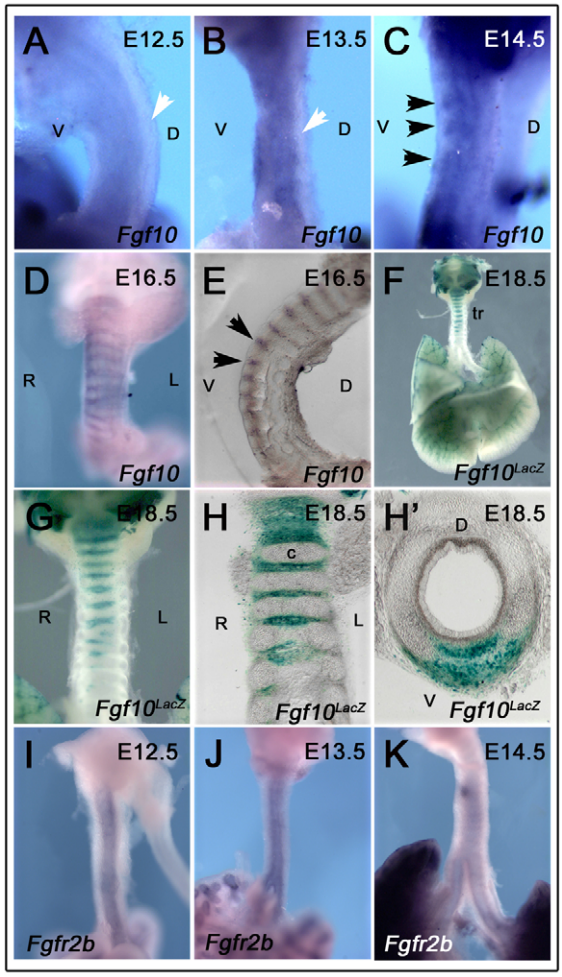

Fig. 1. *Fgf10* and *Fgfr2b* expression pattern in the developing trachea. (**A-E**) Whole-mount in situ hybridization shows *Fgf10* expression in the ventral mesenchyme of the trachea. At E14.5 onwards, we observe a regionalization of the expression in the non-cartilaginous mesenchyme (black arrows in C). The dorsal side of the trachea does not stain for *Fgf10* (white arrows). (E) Sagittal vibratome section of the E16.5 trachea shown in D. Arrows in E indicate *Fgf10* expression in between the cartilage rings. (**F-H'**) This expression pattern is confirmed using the *Fgf10*^{lacZ} at E18.5. (H) Frontal vibratome section of the E18.5 trachea shown in F and G. (H') Transverse vibratome section of the E18.5 trachea shown in F and G. (**I-K**) Whole-mount in situ hybridization shows uniform *Fgfr2b* expression in the tracheal epithelium from E12.5 to E14.5. V, ventral side of the trachea; D, dorsal side; R, right side; L, left side; tr, trachea.

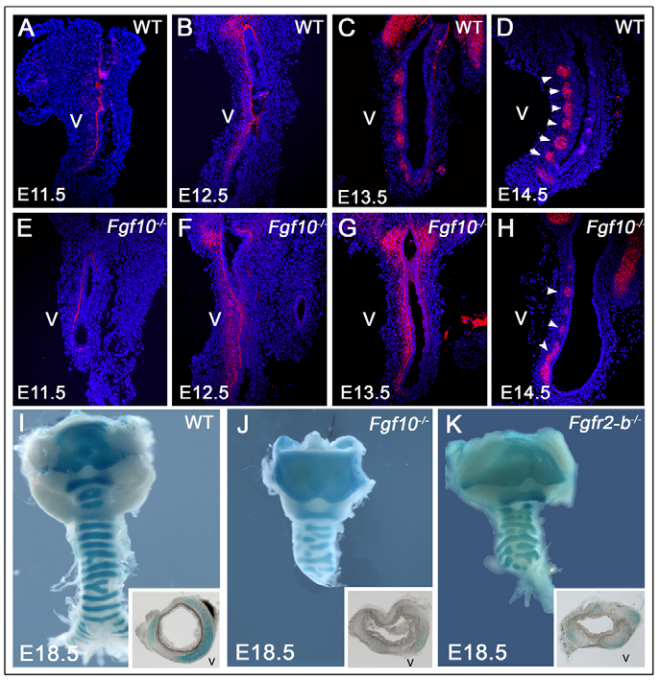

Fig. 2. Time course following the formation of the cartilage rings in *Fgf10*$^{-/-}$ and wild-type tracheas. (**A-H**) E11.5 to E14.5 tracheas, from (A-D) wild-type and (E-H) *Fgf10*-null embryos, were sectioned in a sagittal plane and immunostained for type II collagen. In wild-type tracheas, the patterning of the cartilage rings is established by the condensation of the mesenchyme (white arrows in D) between E12.5 and E14.5. In the *Fgf10*$^{-/-}$ tracheas, the mesenchyme fails to condensate properly at E13.5. Mis-shapen condensations appear 1 day later (white arrows in H). (**I**,**J**) This early developmental defect results in totally disorganized cartilage rings, as seen by Alcian Blue staining of (J) *Fgf10* knockout tracheas at birth compared with (I) wild type. Transverse vibratome sections of the tracheas in I and J (insets) show that the malformations of the cartilage rings observed in the mutant result in a collapse of the airway reminiscent of a tracheomalacia phenotype. (**K**) The same phenotype was observed in E18.5 *Fgfr2b*$^{-/-}$ trachea. V, ventral side; WT, wild type.

segmented (Fig. 2G). By E14.5, the segmentation is present (Fig. 2H), but although the centers of the proximal cartilage condensations in *Fgf10* knockout tracheas are roughly similarly distributed as in the wild type, the condensations are smaller and less uniformly shaped compared with the wild type. Moreover, in the distal part of the trachea type II collagen expression is not segmented at all (Fig. 2H). This early defect of cartilage patterning results in severely disorganized cartilage rings in *Fgf10*$^{-/-}$ tracheas at E18.5 (Fig. 2J). Whereas the tracheal cartilage forms uniform C-shaped rings in the wild type (Fig. 2I), most of the rings do not span an entire C-shape in the *Fgf10*$^{-/-}$ tracheas (Fig. 2J). Transversal vibratome sections of E18.5 tracheas show that the width of the *Fgf10*$^{-/-}$ trachea is roughly the same as in the wild type, yet it is collapsed, reminiscent of the human tracheomalacia phenotype (insets in Fig. 2I,J). This same phenotype is also observed in the *Fgfr2b*$^{-/-}$ tracheas (Fig. 2K, inset), supporting our hypothesis that FGF10 triggers signaling in the epithelium via FGFR2B. Of interest, both mutants have tracheas that are about half the length of a normal trachea, and did not display tracheo-esophageal fistula or tracheal atresia.

Fgf10-null tracheas display normal differentiation but decreased proliferation of the epithelium and mesenchyme

As it is well established that FGF10 plays an important role in controlling the proliferation and/or the differentiation of the epithelium in various organs (Bellusci et al., 1997; Sala et al., 2006; Spencer-Dene et al., 2006; Veltmaat et al., 2006), we next examined these cell decisions in tracheal development.

Hematoxylin and Eosin staining of sagittal sections of E18.5 tracheas shows columnar epithelium in control embryos (Fig. 3A), the height of which seems slightly reduced in *Fgf10*$^{-/-}$ embryos

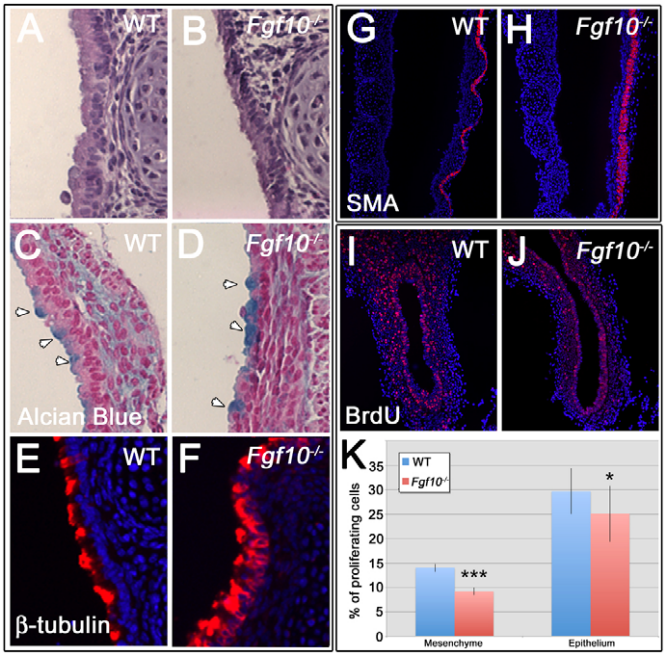

Fig. 3. Differentiation and proliferation analysis in the *Fgf10*$^{-/-}$ and wild-type tracheas at birth. The tracheal lumen is on the left in each panel. (**A**,**B**) Hematoxylin and Eosin staining showing normal pseudo-stratified epithelium in control (A) and *Fgf10*-null (B) tracheas. (**C**,**D**) Alcian Blue staining of the goblet cells (white arrows) in control (C) and *Fgf10*-null (D) tracheas. (**E**,**F**) β-Tubulin immunostaining of ciliated cells in control (E) and *Fgf10*-null (F) tracheas. (**G**,**H**) Smooth muscle actin (SMA) staining of the muscle cells in the dorsal side of control (G) and *Fgf10*-null (H) tracheas. (**I**,**J**) BrdU incorporation in E13.5 wild-type (I) and *Fgf10*$^{-/-}$ (J) tracheas. (**K**) Quantification of BrdU incorporation in mesenchyme and epithelium. Data are mean ± s.e.m. **P*<0.05; ****P*<0.005.

(Fig. 3B). Alcian Blue staining (Fig. 3C,D) and β-tubulin immunostaining (Fig. 3E,F) demonstrate the presence of properly differentiated goblet and ciliated cells, respectively, perhaps with slightly different distributions or shapes in the *Fgf10*$^{-/-}$ tracheas. Immunostaining for smooth muscle actin (SMA) showed no defect in the differentiation of the smooth muscle cells in the dorsal mesenchyme of *Fgf10*$^{-/-}$ tracheas compared with wild-type tracheas (Fig. 3G,H). The section in Fig. 3G is parasagittal, crossing the dorsoventral transition between cartilage and smooth muscle tissue, which explains the undulating pattern of SMA expression. By contrast, the section in Fig. 3H is a midsagittal section showing the straight pattern of SMA expression. In conclusion, *Fgf10*$^{-/-}$ tracheas do not display notable defects in epithelial differentiation.

As *Fgf10*$^{-/-}$ and *Fgfr2b*$^{-/-}$ tracheas are about half the length of wild-type trachea (Fig. 2I-K), we next analyzed the proliferation of the mesenchyme and the epithelium by BrdU incorporation in three pairs of mutant and littermate control embryos from two different mothers. The mutant tracheas showed a 15% decrease in the proliferation of the epithelium (from 29.7% in controls to 25.1%) and a 35% decrease in the proliferation of the mesenchyme (from 14.3% in controls to 9.2%) at E13.5 (Fig. 3I-K). A paired two-tailed *t*-test showed that these decreases were significant in both tissues (*P*=0.017 for the epithelium, and 0.003 for the mesenchyme). At that same stage of development, TUNEL assay showed no apoptosis in both epithelium and mesenchyme of the *Fgf10*$^{-/-}$ tracheas (data not shown), suggesting that the smaller size of mutant tracheas is solely due to a lack of proliferation.

Overexpression of *Fgf10* from E11.5 to E13.5 induces tracheal cartilage ring malformations

In order to explore further the role of FGF10 during the formation of the tracheal cartilage rings, we generated transgenic mice that conditionally overexpressed *Fgf10* under the control of the mesenchymal specific promoter *Dermo1* (Yu et al., 2003) (*tet(O)Fgf10*$^{Dermo\text{-}1}$ hereafter). Overexpression of *Fgf10* was confirmed by feeding doxycycline to females pregnant with E12.5 embryos for 24 hours prior to sacrifice. Compared with control littermates (Fig. 4A), *Fgf10* mRNA is expressed at a higher level in E13.5 *tet(O)Fgf10*$^{Dermo\text{-}1}$ trachea (Fig. 4B). Although such short overexpression did not induce branching of the epithelium (Fig. 4C,D), it did stimulate ectopic SP-C expression on the ventral epithelium (Fig. 4E,F), as previously described by Haytt et al. (Hyatt et al., 2004), which further confirmed that *Fgf10* was overexpressed.

Overexpression was induced for 24 or 48 hours, starting at specific time points during the formation of the cartilage rings (E10.5 to E13.5). The cartilage rings were analyzed at E18.5 by Alcian Blue staining. When induced from E10.5 to E11.5, before the cartilage starts to form, overexpression of *Fgf10* did not alter the patterning of the cartilage rings (Fig. 4G,G′). However, when induced from E11.5 to E13.5, overexpression of *Fgf10* resulted in totally disorganized cartilage rings. We observed an overall reduction of cartilage formation. The cartilage rings fail to form continuous C-shaped rings in the ventral part but fused in the lateral side of the trachea in a proximal-distal fashion. These proximal-distal cartilaginous fusions extend also to the two main bronchi (Fig. 4H,H′). Overexpression for 24 hours between E11.5 and E12.5 or E12.5 and E13.5 also resulted in altered cartilage rings (data not shown). Interestingly, when *Fgf10* is overexpressed after E13.5 for 48 hours, at the time when the cartilage is already patterned, the patterning of the rings is no longer affected (Fig. 4I,I′). Under all conditions, *Fgf10* overexpression did not result in cartilage differentiation in the dorsal side of the trachea, in tracheo-esophageal fistula (data not shown) or in tracheal atresia. The patterning of the cartilage rings of the littermate controls was not affected by the doxycycline treatment (Fig. 4J,J′). Overall, these results demonstrate that E11.5 to E13.5 is the crucial developmental phase where FGF10 controls the patterning of the mesenchyme, allowing the formation of the alternating cartilage segments.

Fgf10 controls the amplitude of periodicity of *Shh* expression in the ventral epithelium of the developing trachea

We next sought to understand the molecular mechanism by which FGF10 (via FGFR2B) regulates the periodicity in tracheal mesenchyme differentiation. Therefore, we examined the expression of *Sox9*, *Bmp4* and *Shh*, known molecular regulators of tracheal cartilage formation (Hatakeyama et al., 2004; Que et al., 2006; Park et al., 2010; Miller et al., 2004), in wild-type and *Fgf10*$^{-/-}$ embryos. We primarily focused our study at E13.5, as this is a crucial stage where cartilage patterning is detectable. We also examined wild-type and mutant tracheas for activated signaling via β-catenin, another known regulator of cartilage formation (Akiyama et al., 2004) and a potential downstream target of FGF10/FGFR2B signaling pathway (Berg et al., 2007), using the *Topgal* reporter line, a *lacZ*-reporter for β-catenin signaling.

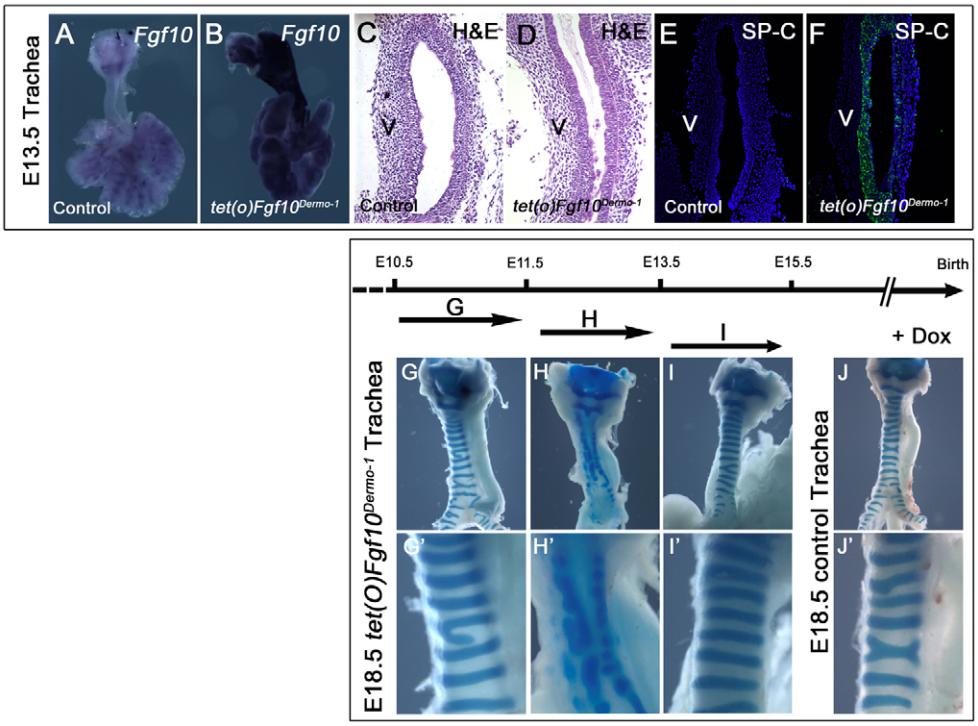

Fig. 4. Overexpression of *Fgf10* between E11.5 and E13.5 results in disruption of the patterning of the cartilage rings. (**A-F**) Validation of *Fgf10* overexpression in *tet(O)Fgf10*$^{Dermo\text{-}1}$ tracheas. (A,B) Whole-mount in situ hybridization for *Fgf10* in wild type (A) and *tet(o)Fgf10*$^{Dermo\text{-}1}$ (B) induced from E12.5 to E13.5 demonstrates overexpression of *Fgf10* in the mesenchyme. (C,D) Hematoxylin and Eosin staining of wild type (C) and *tet(O)Fgf10*$^{Dermo\text{-}1}$ (D) from E11.5 to E13.5, demonstrating that this short overexpression did not result in branching of the epithelium. (E,F) *Fgf10* overexpression induces SP-C expression in the ventral epithelium of *tet(O)Fgf10*$^{Dermo\text{-}1}$ trachea (F, green) induced from E12.5 to E13.5. (**G-J'**) Low (G-J) and high (G'-J') magnification pictures of mutant (G-I') and wild-type (J,J') tracheas. Overexpression of *Fgf10* was induced in *tet(O)Fgf10*$^{Dermo\text{-}1}$ tracheas for 24 or 48 hours at specific time points during cartilage formation. The mutant tracheas were collected at birth, stained with Alcian Blue and compared with control littermate (J,J'). (G,G') *Fgf10* overexpression from E10.5 to E11.5 does not alter the patterning of the cartilage rings. (H,H') Induction between E11.5 and E13.5 results in malformation of the cartilage rings. The cartilage fails to form C-shaped rings and some rings fuse in a proximal-distal manner. (I,I') Overexpression from E13.5 to E15.5 does not affect the patterning of the cartilage rings.

Inactivation of *Fgf10* did not affect the expression level of *Sox9* and *Bmp4* mRNA (Fig. 5A-D) or that of *Topgal* (Fig. 5E,F). However, we did observe a change in the pattern of *Shh* expression (Fig. 6).

Using whole-mount in situ hybridization, we followed the expression pattern of *Shh* during a wider time-window of tracheal development. In wild types, *Shh* is uniformly expressed in the entire tracheal epithelium at E11.5 and E12.5 either along the left/right axis or the ventral/dorsal axis (Fig. 6A,B, respectively). At E13.5, although remaining uniformly expressed throughout the dorsal tracheal epithelium, *Shh* acquires a periodic expression pattern in the ventral epithelium (Fig. 6C). This periodic *Shh* expression pattern is more pronounced at E14.5 (Fig. 6D). *Shh* expression in the ventral side seems lower than in the dorsal side. To further illustrate the periodicity of *Shh* expression, we measured the hybridization signal for *Shh* mRNA along a precise location on the ventral side (green line) using pixel intensity in digital photographs of tracheas (Fig. 6E-G). In wild-type trachea, the presence of minima and maxima in pixel intensity (illustrated as double-headed arrows in the green line in Fig. 6G) indicates a periodicity of *Shh* expression in the ventral side of the trachea. Quantitative analysis indicates that the average peak-to-peak amplitude in intensity is about 22 pixels (average minimum intensity=37 pixels; average maximum intensity=59 pixels). By contrast, *Shh* expression in the dorsal side is uniform. The dorsal expression of *Shh* is also stronger than ventral confirming the previous observation. This ventral periodic expression at E13.5 correlates with a ventral periodic expression of type II collagen at that same developmental stage (Fig. 6H). Macroscopic analysis of E13.5 *Fgf10*$^{-/-}$ tracheas after whole-mount in situ hybridization suggests a reduced amplitude in periodicity of *Shh* expression in the ventral side. In addition, the difference in *Shh* expression levels between ventral and dorsal sides appears reduced (Fig. 6I). Measurement of the pixel intensities revealed that dorsal epithelial *Shh* expression is indeed still higher than ventrally. Furthermore, periodicity in *Shh* expression was still detected in the ventral epithelium (green line in Fig. 6K), but the average peak-to-peak amplitude is reduced to only 13.5 pixels (average minimum intensity=68.5; average maximum intensity=82). Interestingly, *Shh* expression in the dorsal epithelium is less uniform along the anterior-posterior axis. The reduced amplitude and regularity of periodicity of ventral *Shh* expression in *Fgf10*$^{-/-}$ trachea is associated with an absence of periodicity of type II collagen expression (Fig. 6L). In *tet(O)Fgf10*$^{Dermo\text{-}1}$ tracheas that overexpress *Fgf10*, *Shh* expression levels progressively increase along the ventrodorsal axis but remain uniform along the anteroposterior axis (Fig. 6M-O). The complete absence of periodicity of *Shh* expression in the ventral epithelium (Fig. 6M-O) is again associated with a loss of periodicity of type II collagen expression (Fig. 6P).

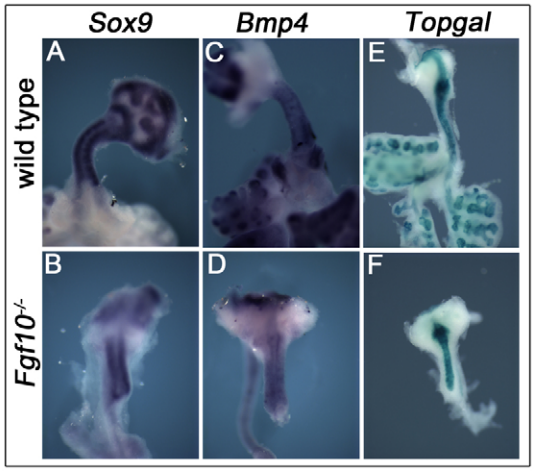

Fig. 5. Inactivation of *Fgf10* does not affect the *Bmp4/Sox9* signaling pathway nor β-catenin activation in the epithelium. (**A**,**B**) Whole-mount in situ hybridization for *Sox9* in E13.5 wild-type (A) and *Fgf10*$^{-/-}$ (B) tracheas. (**C**,**D**) Whole-mount in situ hybridization for *Bmp4* in E13.5 wild-type (C) and *Fgf10*$^{-/-}$ (D) tracheas. (**E**,**F**) β-Catenin activation in wild-type (E) and *Fgf10*$^{-/-}$ (F) tracheas using the *Topgal* reported line, a *lacZ* reporter for β-catenin signaling.

These data indicate that mesenchymal *Fgf10* is not required for epithelial *Shh* expression per se, and strongly suggest that the expression of *Fgf10* must be critically balanced to allow for periodicity of *Shh* expression. It is interesting to note that *Shh* expression in the esophageal epithelium is unchanged in the *Fgf10*$^{-/-}$ mutants (Fig. 6I), and completely lost in the *tet(O)Fgf10*$^{Dermo\text{-}1}$ mutants (Fig. 6M), suggesting that FGF10 negatively regulates *Shh* transcription in the esophagus.

Changes in periodicity of epithelial *Shh* expression cause defects in mesenchyme condensation, resulting in cartilage ring malformations

To further explore the role of SHH in tracheal cartilage formation, we made use of the previously reported *Ttf-1*^{cre} (or *Nkx2.1*^{cre}) driver line either to delete or overexpress *Shh* in the tracheal epithelium. To verify the activity of this line, we crossed the *Ttf-1*^{cre} driver line with the *Rosa26R* reporter line containing a floxed *lacZ* gene in the *Rosa26*-locus (Soriano, 1999). As expected, β-galactosidase was specifically expressed in the epithelium (Fig. 7A). Sagittal sectioning of the trachea indicates that the *Ttf-1* promoter drives the expression of Cre recombinase mostly in the ventral epithelium and at lower level in the dorsal epithelium (Fig. 7B). Next, we used this line to specifically inactivate [*Ttf-1*^{cre}*; Shh*$^{f/f}$] or conditionally overexpress [*rtTA*^{flox}*-tet(O)Shh,* hereafter called *tet(O)Shh*$^{Ttf\text{-}1}$] *Shh* expression in the tracheal epithelium. We validated *Shh* overexpression in the epithelium of E13.5 *tet(O)Shh*$^{Ttf\text{-}1}$ tracheas by whole-mount in situ hybridization for *Shh* (Fig. 7C,D) and patched 1 (*Ptch1*), a receptor and downstream target of SHH (Fig. 7E,F).

Shh inactivation results in low level of type II collagen expression in E13.5 trachea (Fig. 7H) and lack of segmentation compared with wild types (Fig. 7G). Compared with the uniform pattern of alternating C-shaped cartilage rings in wild types (Fig. 7J,J′) at E18.5, [*Ttf-1*^{cre}*; Shh*$^{f/f}$] tracheas show strong reduction of cartilage formation. Rudimentary rings that formed are truncated at the ventral midline (Fig. 7K,K′), similar to what we observed in *Fgf10* overexpressing trachea. It is interesting to note that, despite an absence of supporting rings, the lumen of the trachea did not collapse (inset in Fig. 7K). Overexpression of *Shh* in *tet(O)Shh*$^{Ttf\text{-}1}$ tracheas from E12.5 to E13.5 upon exposure of the pregnant females to doxycycline food results at E13.5 in sustained type II collagen deposition with absence of segmentation (Fig. 7I), similar to the *Fgf10*$^{-/-}$ tracheal phenotype (Fig. 2G, Fig. 6L). At E18.5, transient *Shh* overexpression during the E12.5/E13.5 time frame induced a strong differentiation of the mesenchyme into cartilage, resulting in mis-shaped rings. The cartilage rings fuse laterally (Fig. 7L,L′). This anomaly resulted in a narrowing of the lumen of the trachea (inset in Fig. 7L) compared with the lumen of a wild-type trachea (inset in Fig. 7J). Similar to the *Fgf10*-null and over-expressing mutants, *Shh* deletion and overexpressing mutants do not form cartilage dorsally, and do not display tracheo-esophageal fistula or tracheal atresia. To demonstrate that *Fgf10* and *Shh* interact at the genetic level, we have generated wild type, single heterozygous, as well as double heterozygous (*Fgf10*$^{+/-}$*; Shh*$^{+/-}$) tracheas at E18.5 and determined the formation of the cartilage by Alcian Blue staining. Double heterozygous tracheas (n=5) demonstrate significant cartilage defects not observed in single heterozygous (n=5) or wild-type tracheas (n=5). These defects include aborted rings and mis-shapen rings (Fig. 8). These defects are reminiscent of the defects observed in *Fgf10*-null mutant and indicate that there is indeed a genetic interaction between *Fgf10* and *Shh*.

DISCUSSION

As periodicity in the tracheal cartilage is essential for an optimal breathing function, we sought to understand how periodic patterning of the tracheal cartilage is established. Using mouse embryos, we show here that the ventral tracheal mesenchyme expresses type II collagen, an early marker of cartilage formation, as a continuum along the proximal-distal axis starting at E11.5. Expression becomes periodic around E13.5. We found that perturbation of *Fgf10* expression levels results in incomplete and irregularly shaped cartilaginous C-shaped rings. We therefore investigated its role in tracheal cartilage formation in more detail.

We did not detect any *Fgf10* mRNA expression in the trachea at E11.5, when cartilaginous differentiation of the ventral tracheal mesenchyme has already begun. Moreover, while *Fgf10* expression is detectable in the ventral tracheal mesenchyme from E12.5 onwards, it is continuous along the proximal-distal axis at that time and only becomes periodic at around E14.5, at least one day later than periodic pre-cartilaginous condensations are observed in the ventral tracheal mesenchyme. At that time, *Fgf10* is expressed in between those condensations. In *Fgf10*$^{-/-}$ mutants, cartilage forms as incomplete rings. Together, these data demonstrate that *Fgf10* expression is neither required for the induction of cartilaginous differentiation of the tracheal mesenchyme, nor for the establishment or maintenance of periodicity within the tracheal mesenchyme. However, *Fgf10* is required for the proper patterning of tracheal mesenchymal differentiation, i.e. for complete and properly shaped cartilage rings. Using mutant mice conditionally overexpressing *Fgf10* in the mesenchyme, we established that the critical time-window for this function of *Fgf10* is between E11.5 and E13.5, which nicely coincides with the time-frame during which periodic patterning of the tracheal mesenchyme is observed.

Interestingly, aside from the shorter tracheal length (and lack of lung development) in *Fgf10*$^{-/-}$ mutants, the tracheal cartilage phenotypes of constitutive *Fgf10*-null mutants and mutants

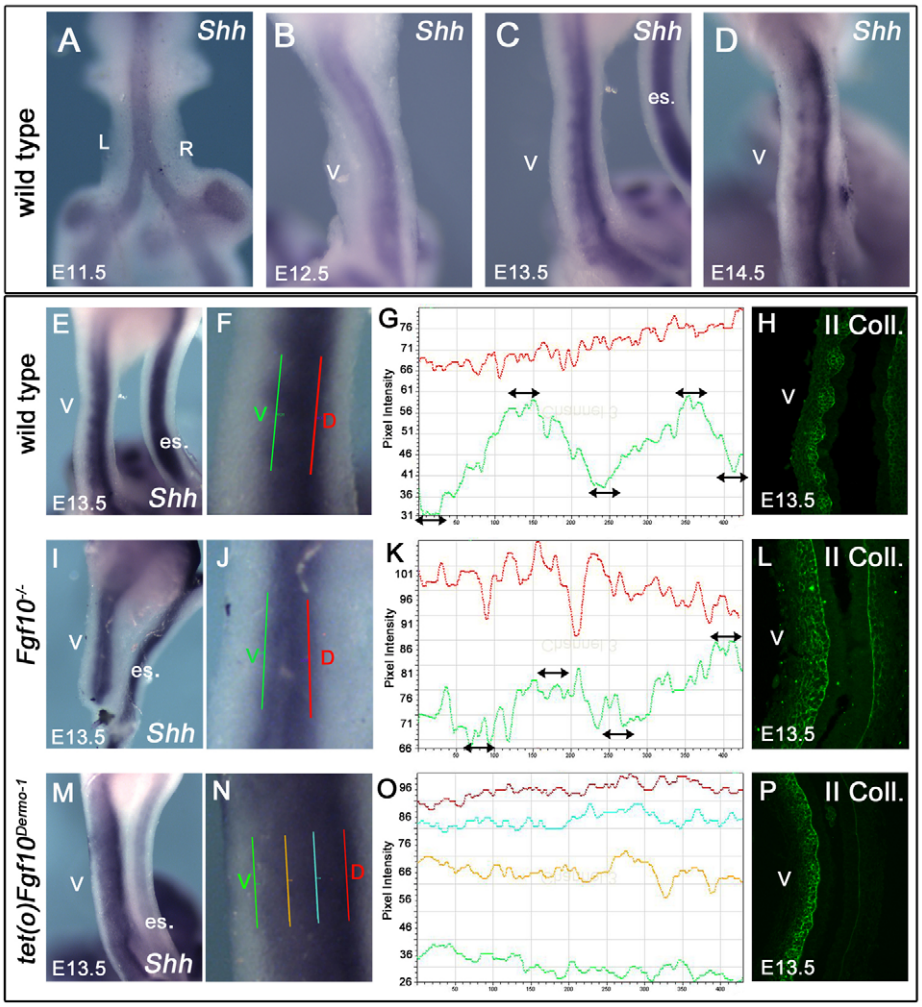

Fig. 6. *Fgf10* controls the amplitude of periodicity of *Shh* expression in the ventral epithelium of the developing trachea. (**A-D**) Whole-mount in situ hybridization for *Shh* in wild-type embryonic tracheas between E11.5 and E14.5. (C,D) Starting at E13.5, *Shh* is expressed in a periodic fashion in the ventral epithelium, whereas it is uniformly expressed in the dorsal epithelium. There is strong *Shh* expression in the esophagus. (**E-G**) Signal quantification (G) of *Shh* expression in wild-type trachea (E) along the two lines shown in F. We observe an oscillation of the signal in the ventral side of the E13.5 trachea (green line), whereas the signal is uniform and stronger in the dorsal side (red line). (**H**) Periodic expression pattern of type II collagen in the ventral side of E13.5 wild-type trachea. (**I-K**) Signal quantification (K) of *Shh* expression in E13.5 *Fgf10*$^{-/-}$ trachea (I) along the two lines shown in J. Although an oscillation in the ventral side (green line) is present, the pattern and the amplitude of the signal is less defined when compared with wild-type trachea (green line in G). *Shh* is evenly expressed throughout the esophageal epithelium. (**L**) Loss of periodic expression pattern of type II collagen in the ventral side of E13.5 *Fgf10*-null trachea. (**M-O**) Signal quantification (O) of *Shh* expression in E13.5 *tet(O)Fgf10*$^{Dermo\text{-}1}$ trachea (M) along the four lines shown in N. After 24 hours of *Fgf10* overexpression, *tet(O)Fgf10*$^{Dermo\text{-}1}$ tracheas show uniform and low *Shh* expression in the ventral (green line) epithelium and normal levels in the dorsal epithelium (red line). The yellow and cyan lines demonstrate a progressively increased, but still uniform, expression of *Shh* from ventral to dorsal. *Shh* expression in the esophagus disappeared. (**P**) Loss of periodic expression pattern of type II collagen in the ventral side of E13.5 *tet(O)Fgf10*$^{Dermo\text{-}1}$ trachea. Black double-headed arrows indicate minimas and maximas of *Shh* expression. V, ventral side of the trachea; L, left side; R, right side; es., esophagus.

overexpressing *Fgf10* during a 48-hour period between E11.5 and E13.5 share a common feature: the cartilage rings are induced but they are truncated. The rings do not extend far enough dorsally, resulting in a flaccid tracheal support, characteristic of tracheomalacia in humans. In both gain- and loss-of-function of *Fgf10*, we found a change in localized expression of *Shh*, a key regulator of cartilage formation (Miller et al., 2004). We propose that the FGF10-controlled segmentation of *Shh* expression is crucial for the proper patterning of the cartilage and that changes in the expression level of *Shh* along the proximal-distal axis will directly impact the integrity of the rings being formed. The proposed interaction between these two signaling pathways is supported at the genetic level as double heterozygous *Fgf10*$^{+/-}$;*Shh*$^{+/-}$ tracheas display both aborted rings and misshapen rings, a defect not observed in wild-type and single heterozygous (Fig. 8). Collectively, these data strongly suggest that the *Fgf10* expression level needs to be within a crucial range to allow for proper patterning of the tracheal mesenchyme. Importantly, ablation or temporal overexpression of mesenchymal *Fgf10* does not lead to tracheo-esophageal fistula, which sometimes accompanies tracheomalacia in humans.

As FGFR2B is the main receptor for FGF10 expressed on epithelial cells (De Moerlooze et al., 2000) and, moreover, the tracheal phenotype of *Fgfr2b*$^{-/-}$ mutants is strikingly similar to that

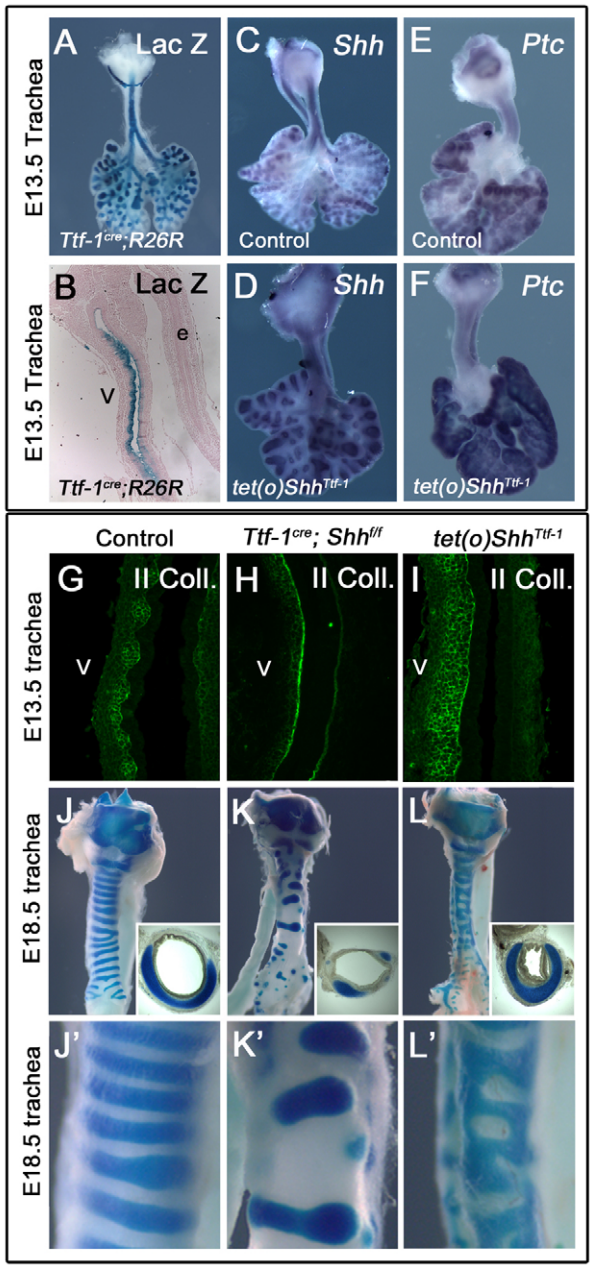

Fig. 7. Gain- or loss-of-function of *Shh* induces severe malformation of the tracheal cartilage rings at E18.5. (**A**,**B**) β-Galactosidase staining of [*Ttf-1*^{cre}*;R26R]* tracheas demonstrates the specific epithelial expression of the *Ttf-1* promoter. (**C**,**D**) *Shh* in situ hybridization in control and *tet(O)Shh*^{Ttf1} tracheas induced for 24 hours, demonstrating increased *Shh* expression. (**E**,**F**) In situ hybridization for patched 1 (*Ptch1*) in control and *tet(O)Shh*^{Ttf1} tracheas, demonstrating increased SHH activity. (**G-I**) Type II collagen immunofluorescence staining. (G) In E13.5 control trachea, the pattern of the pre-cartilaginous mesenchymal condensation is being established. (H) In E13.5 [*Ttf-1*^{cre}*;Shh*$^{f/f}$] trachea, where *Shh* has been specifically inactivated in the epithelium, type II collagen expression is very low and the mesenchyme fails to condensate. (I) In E13.5 *tet(O)shh*$^{Ttf-1}$ trachea, overexpressing *Shh* for 24 hours leads to strong expression of type II collagen but absence of mesenchymal condensation, as seen in the *Fgf10*-null trachea (Fig. 2G). (**J-L'**) Alcian Blue staining of E18.5 control and mutant tracheas (J-L) and respective high-magnification pictures (J'-L'). (J,J') E18.5 control trachea demonstrates normal patterning of the cartilage rings. Vibratome cross-section of a wild-type trachea shows normal opening of the lumen (inset in J). (K,K') E18.5 [*Ttf-1*^{cre}*;Shh*$^{f/f}$] shows a strong reduction of cartilage differentiation. The few rings forming are mis-shaped. Surprisingly, vibratome cross-section of [*Ttf-1*^{cre}*;Shh*$^{f/f}$] trachea shows normal opening of the lumen (inset in K). (L,L') E18.5 *tet(O)shh*$^{Ttf-1}$ trachea, overexpressing *Shh* for 24 hours from E12.5 to E13.5 specifically in the epithelium, shows disorganized rings that fuse in a proximal-distal fashion. Vibratome cross-section of *tet(O)shh*$^{Ttf-1}$ trachea demonstrates a narrowing of the lumen (inset in L).

of *Fgf10*$^{-/-}$ mutants, we conclude that in a normal situation, FGF10 exerts its role in mesenchymal patterning via activation of the tracheal epithelium. This is very different from the role we established for FGF10 in a mouse model of Apert syndrome (Tiozzo et al., 2009), in which FGF10 activates ectopically expressed FGFR2B receptors in the mesenchyme, resulting in cartilaginous overgrowth. Although those previous data indicate that FGF signaling in the mesenchyme can induce its differentiation into cartilage, our current data show that FGF10 is normally not an autocrine activator of FGF signaling in the mesenchyme, but an activator of FGFR2B signaling in the tracheal epithelium. Interestingly, this activation seems to have no or little importance for the differentiation of the epithelium itself, as we observed the presence of both ciliated and goblet cells in trachea of *Fgf10*$^{-/-}$ mutants. Thus, the main role of FGF10 during this early developmental stage may be to coordinate mesenchymal patterning, using the epithelium as an intermediate.

Besides FGF signaling, β-catenin signaling, BMP4 and SHH are known to be involved in tracheal cartilage formation (Akiyama et al., 2004; Hatakeyama et al., 2004; Park et al., 2010). We found that β-catenin signaling and *Bmp4* expression are not changed in *Fgf10*$^{-/-}$ mutants. Although recombinant FGF10 upregulates *Bmp4* expression in the tracheal epithelium in tracheo-pulmonary organotypic cultures in vitro (Hyatt et al., 2004), FGF10 is apparently not required for *Bmp4* expression in vivo. We did not observe a change in *Sox9* expression either, which was unexpected because SOX9 is implicated in cartilage formation mediated by β-catenin signaling, BMP4 and SHH (Akiyama et al., 2004; Hatakeyama et al., 2004; Park et al., 2010). We cannot exclude the possibility that a change was present, but we may have failed to observe it as it might be obscured due to the partial formation of cartilage rings in the mutants. Alternatively, changes may have occurred at the translational or post-translational level instead of at the RNA level.

Interestingly, although *Shh* expression in the epithelium normally becomes periodic at around E13.5, concomitant with mesenchymal patterning, periodicity of *Shh* was less pronounced in *Fgf10*$^{-/-}$ mutants and was absent in *Fgf10* overexpressing mutants. This is of particular interest, as the gene encoding PTCH1, a transducer and transcriptional target of SHH, is expressed in the pre-cartilaginous condensations at E13.5 (Miller et al., 2004); SHH has also been shown to control the *Sox9* expression pattern (Park et al., 2010). Indeed, we observed defects in cartilage formation in mutants with constitutive ablation of *Shh* in the tracheal epithelium or with temporal overexpression between E11.5 and E13.5 in that tissue. SHH is required for the differentiation and the proper patterning of the cartilaginous differentiation of the mesenchyme. As for *Fgf10*, the level of *Shh* expression needs to be within a critical range for proper patterning of tracheal cartilage. This result indicates that neither SHH nor FGF10 is an instructive signal for cartilage formation. Interestingly, disruption of dorsoventral

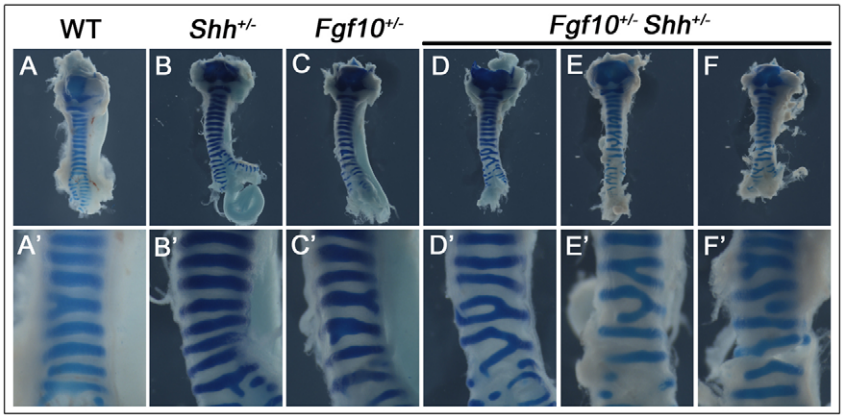

Fig. 8. Genetic interaction between *Shh* and *Fgf10*. Low and high magnification of wild-type (**A**,**A′**), *Shh*$^{+/-}$ (**B**,**B′**), *Fgf10*$^{+/-}$ (**C**,**C′**) and *Fgf10*$^{+/-}$;*Shh*$^{+/-}$ (**D-F′**) tracheas at E18.5 stained with Alcian Blue to visualize the cartilage rings. Regularly spaced and mostly complete rings are present in wild-type and single heterozygous tracheas (A-C′). By contrast, double heterozygous tracheas (D-F′) display both aborted rings and mis-shapen rings.

partitioning of *Fgf10* and *Shh* expression does not alter dorsoventral patterning of the trachea in terms of separation of the muscle lineage on the dorsal side and cartilage lineage on the ventral side.

Establishment of complex patterns during embryonic development is a major interest in the field of developmental biology. Two conceptual developmental models have been proposed to explain the formation of repetitive patterns. Of these, the clock and wave-front model involves the cyclic expression of specific genes resulting in a repetitive pattern (Cooke and Zeeman, 1976). In contrast to other periodic patterns, such as somite or hair follicle formation, where the new structures form sequentially, the tracheal cartilaginous segments seem to be induced simultaneously and mature over an extended period of time (between E13.5 and E14.5). In addition, we did not observe any cyclic expression of *Fgf10* or *Shh*. These pieces of evidence seem therefore to argue against a clock-and-wavefront model underlying tracheal cartilage formation. In the alternative reaction-diffusion model proposed by Alan Turing, two morphogens – an activator and the activator-dependent inhibitor – establish periodic patterning during development (Turing, 1952; Gierer and Meinhartd, 1972). We wondered whether Turing's model, with SHH and FGF10 acting as the activating and inhibiting morphogens, would apply to tracheal cartilage formation. We demonstrated that *Shh* is expressed prior to *Fgf10* in the trachea (Figs 1 and 6) and that *Fgf10* expression represses *Shh* expression (Fig. 6). In addition, *Shh* expression becomes periodic only after *Fgf10* expression becomes detectable, and *Fgf10* expression becomes periodic only after *Shh* expression has become periodic. One could propose SHH as an activator and FGF10 as the activator-dependent inhibitor, the periodicity of which reinforces the periodicity of *Shh* expression, although it remains unclear how the initial periodicity of *Shh* expression is achieved. However, removal of the activator or inhibitor in Turing's model would result in the complete absence of periodicity, i.e. either no cartilage formation at all or formation of a continuous cartilaginous sleeve. We still observed residual periodicity in the tracheal cartilage in our loss- and gain-of-function models for *Fgf10* and *Shh*. Thus, although it remains of interest to determine whether tracheal cartilage rings form according to Turing's model, our current data would exclude FGF10 and SHH as an activator-inhibitor pair of morphogens in this model.

In conclusion, we show for the first time that both *Fgf10* and *Shh* expression levels are crucial between E11.5 and E13.5 for tracheal cartilage patterning in the mouse embryo. The similarity in tracheal phenotypes between *Fgf10*$^{-/-}$ and *Fgfr2b*$^{-/-}$ embryos strongly suggest that FGF10 exerts its role in cartilage formation via activation of FGFR2B in the epithelium. Although this signaling is not required for epithelial differentiation itself, it may be a regulator of periodic *Shh* expression in the epithelium. The residual and irregular formation of cartilage rings in the absence of *Fgf10* indicate that this molecule does not act in the induction of periodicity, but rather in the fine-tuning of it. Finally, we show that reduced or elevated expression of *Fgf10* and *Shh* did not induce any tracheo-esophageal fistula or atresia. This is in sharp contrast with tracheo-esophageal fistula co-occurring with tracheomalacia, owing to perturbations of BMP signaling (Que et al., 2006), and underscores the distinct role played by FGF10/SHH versus BMP signaling, in tracheal malformations. Thus, our current results not only provide novel insights in the mechanism of action of *Fgf10* and *Shh* on normal tracheal cartilage formation, but may also provide helpful diagnostic criteria for the development and application of future molecular therapies to prevent or correct congenital tracheal cartilage defects.

Acknowledgements

We thank Drs N. Itoh, R. Kelly, D. Ornitz, J. Whitsett and P. Minoo for the kind gifts of the mice used in this project. F.S. acknowledges the financial support from an intramural grant from Childrens Hospital Los Angeles and the California Institute of Regenerative Medicine (CIRM). J.V. acknowledges fellowships from the California Breast Cancer Research Program 10-FB-0116 and Childrens Hospital Los Angeles. T.G. acknowledges funding from CIRM (RN2-00946-1). D.W. acknowledges funding from NIH (HL44060, HL44977, HL60231, HL75773) and the Pasadena Guild Endowment of Childrens Hospital Los Angeles. S.B. acknowledges the funding from NIH (HL086322 and HL074832) as well as from the Excellence Cluster in Cardio-Pulmonary System. Deposited in PMC for release after 12 months.

Competing interests statement

The authors declare no competing financial interests.

References

Akiyama, H., Lyons, J. P., Mori-Akiyama, Y., Yang, X., Zhang, R., Zhang, Z., Deng, J. M., Taketo, M. M., Nakamura, T., Behringer, R. R. et al. (2004). Interactions between Sox9 and beta-catenin control chondrocyte differentiation. *Genes Dev.* **18**, 1072-1087.

Austin, J. and Ali, T. (2003). Tracheomalacia and bronchomalacia in children: pathophysiology, assessment, treatment and anaesthesia management. *Paediatr. Anaesth.* **13**, 3-11.

Bellusci, S., Grindley, J., Emoto, H., Itoh, N. and Hogan, B. L. (1997). Fibroblast growth factor 10 (FGF10) and branching morphogenesis in the embryonic mouse lung. *Development* **124**, 4867-4878.

Belteki, G., Haigh, J., Kabacs, N., Haigh, K., Sison, K., Costantini, F., Whitsett, J., Quaggin, S. E. and Nagy, A. (2005). Conditional and inducible transgene expression in mice through the combinatorial use of Cre-mediated recombination and tetracycline induction. *Nucleic Acids Res.* **33**, e51.

Berg, T., Rountree, C. B., Lee, L., Estrada, J., Sala, F. G., Choe, A., Veltmaat, J. M., De Langhe, S., Lee, R., Tsukamoto, H. et al. (2007). Fibroblast growth factor 10 is critical for liver growth during embryogenesis and controls hepatoblast survival via beta-catenin activation. *Hepatology* **46**, 1187-1197.

Clark, J. C., Tichelaar, J. W., Wert, S. E., Itoh, N., Perl, A. K., Stahlman, M. T. and Whitsett, J. A. (2001). FGF-10 disrupts lung morphogenesis and causes pulmonary adenomas in vivo. *Am. J. Physiol. Lung Cell Mol. Physiol.* **280**, L705-L715.
Cooke, J. and Zeeman, E. C. (1976). A clock and wavefront model for control of the number of repeated structures during animal morphogenesis. *J. Theor. Biol.* **58**, 455-476.
DasGupta, R. and Fuchs, E. (1999). Multiple roles for activated LEF/TCF transcription complexes during hair follicle development and differentiation. *Development* **126**, 4557-4568.
De Moerlooze, L., Spencer-Dene, B., Revest, J. M., Hajihosseini, M., Rosewell, I. and Dickson, C. (2000). An important role for the IIIb isoform of fibroblast growth factor receptor 2 (FGFR2) in mesenchymal-epithelial signalling during mouse organogenesis. *Development* **127**, 483-492.
Gierer, A. and Meinhardt, H. (1972). A theory of biological pattern formation. *Kybernetik* **12**, 30-39.
Goldring, M. B., Tsuchimochi, K. and Ijiri, K. (2006). The control of chondrogenesis. *J. Cell. Biochem.* **97**, 33-44.
Hatakeyama, Y., Tuan, R. S. and Shum, L. (2004). Distinct functions of BMP4 and GDF5 in the regulation of chondrogenesis. *J. Cell. Biochem.* **91**, 1204-1217.
Ho, A. S. and Koltai, P. J. (2008). Pediatric tracheal stenosis. *Otolaryngol. Clin. North Am.* **41**, 999-1021.
Hyatt, B. A., Shangguan, X. and Shannon, J. M. (2004). FGF-10 induces SP-C and Bmp4 and regulates proximal-distal patterning in embryonic tracheal epithelium. *Am. J. Physiol. Lung Cell. Mol. Physiol.* **287**, L1116-L1126.
Kay, D. J. and Goldsmith, A. J. (2006). Laryngomalacia: a classification system and surgical treatment strategy. *Ear Nose Throat J.* **85**, 328-331, 336.
Kelly, R. G., Brown, N. A. and Buckingham, M. E. (2001). The arterial pole of the mouse heart forms from Fgf10-expressing cells in pharyngeal mesoderm. *Dev. Cell* **1**, 435-440.
Miller, L. A., Wert, S. E., Clark, J. C., Xu, Y., Perl, A. K. and Whitsett, J. A. (2004). Role of Sonic hedgehog in patterning of tracheal-bronchial cartilage and the peripheral lung. *Dev. Dyn.* **231**, 57-71.
Ohuchi, H. (2000). Roles for FGF-FGFR signaling during vertebrate development. *Hum. Cell* **13**, 169-175.
Park, J., Zhang, J. J., Moro, A., Kushida, M., Wegner, M. and Kim, P. C. (2010). Regulation of Sox9 by Sonic Hedgehog (Shh) is essential for patterning and formation of tracheal cartilage. *Dev. Dyn.* **239**, 514-526.
Que, J., Choi, M., Ziel, J. W., Klingensmith, J. and Hogan, B. L. (2006). Morphogenesis of the trachea and esophagus: current players and new roles for noggin and Bmps. *Differentiation* **74**, 422-437.
Sala, F. G., Curtis, J. L., Veltmaat, J. M., Del Moral, P. M., Le, L. T., Fairbanks, T. J., Warburton, D., Ford, H., Wang, K., Burns, R. C. et al. (2006). Fibroblast growth factor 10 is required for survival and proliferation but not differentiation of intestinal epithelial progenitor cells during murine colon development. *Dev. Biol.* **299**, 373-385.
Sandell, L. J., Nalin, A. M. and Reife, R. A. (1994). Alternative splice form of type II procollagen mRNA (IIA) is predominant in skeletal precursors and non-cartilaginous tissues during early mouse development. *Dev. Dyn.* **199**, 129-140.
Sekine, K., Ohuchi, H., Fujiwara, M., Yamasaki, M., Yoshizawa, T., Sato, T., Yagishita, N., Matsui, D., Koga, Y., Itoh, N. et al. (1999). Fgf10 is essential for limb and lung formation. *Nat. Genet.* **21**, 138-141.
Soriano, P. (1999). Generalized lacZ expression with the ROSA26 Cre reporter strain. *Nat. Genet.* **21**, 70-71.
Spencer-Dene, B., Sala, F. G., Bellusci, S., Gschmeissner, S., Stamp, G. and Dickson, C. (2006). Stomach development is dependent on fibroblast growth factor 10/fibroblast growth factor receptor 2b-mediated signaling. *Gastroenterology* **130**, 1233-1244.
Tiozzo, C., De Langhe, S., Carraro, G., Alam, D. A., Nagy, A., Wigfall, C., Hajihosseini, M. K., Warburton, D., Minoo, P. and Bellusci, S. (2009). Fibroblast growth factor 10 plays a causative role in the tracheal cartilage defects in a mouse model of Apert syndrome. *Pediatr. Res.* **66**, 386-390.
Turing, A. M. (1952). The chemical basis of morphogenesis. *Philos. Trans. R. Soc. Lond. B Biol. Sci.* **237**, 37-72.
Veltmaat, J. M., Relaix, F., Le, L. T., Kratochwil, K., Sala, F. G., van Veelen, W., Rice, R., Spencer-Dene, B., Mailleux, A. A., Rice, D. P. et al. (2006). Gli3-mediated somitic Fgf10 expression gradients are required for the induction and patterning of mammary epithelium along the embryonic axes. *Development* **133**, 2325-2335.
Winnier, G., Blessing, M., Labosky, P. A. and Hogan, B. L. (1995). Bone morphogenetic protein-4 is required for mesoderm formation and patterning in the mouse. *Genes Dev.* **9**, 2105-2116.
Yu, K., Xu, J., Liu, Z., Sosic, D., Shao, J., Olson, E. N., Towler, D. A. and Ornitz, D. M. (2003). Conditional inactivation of FGF receptor 2 reveals an essential role for FGF signaling in the regulation of osteoblast function and bone growth. *Development* **130**, 3063-3074.